Report No. 270

UNIVERSITY OF BRISTOL

DEPARTMENT OF
AERONAUTICAL ENGINEERING

SHEAR DIFFUSION IN SANDWICH SPECIMENS HAVING GLASS REINFORCED PLASTIC FACE PLATES WITH PAPER HONEYCOMB CORES

by

A. M. AHMAD MUSTAPHA
and
C. K. LIEW

Report submitted for the Degree of
B.Sc. in Engineering with Honours.

JUNE 1981

MSG DIA CROL PROCESSING-LAST INPUT IGNORED

-- 1 OF 1
-- ***DTIC DOES NOT HAVE THIS ITEM***
-- 1 - AD NUMBER: D435762
-- 5 - CORPORATE AUTHOR: BRISTOL UNIV (ENGLAND) DEPT OF AERONAUTICAL
-- ENGINEERING
-- 6 - UNCLASSIFIED TITLE: SHEAR DIFFUSION IN SANDWICH SPECIMENS
-- HAVING GLASS REINFORCED PLASTIC PLATES WITH PAPER HONEYCOMB CORES,
--10 - PERSONAL AUTHORS: MUSTAPHA,A. M. ;LIEW,C. K. ;
--11 - REPORT DATE: JUN , 1981
--12 - PAGINATION: 48P
--14 - REPORT NUMBER: BU-270
--20 - REPORT CLASSIFICATION: UNCLASSIFIED
--21 - SUPPLEMENTARY NOTE: B. S. THESIS.
--22 - LIMITATIONS (ALPHA): APPROVED FOR PUBLIC RELEASE; DISTRIBUTION
-- UNLIMITED. AVAILABILITY: NATIONAL TECHNICAL INFORMATION SERVICE,
-- SPRINGFIELD, VA. 22161. N82-19327.
--33 - LIMITATION CODES: 1 24
--******
-- END OF DISPLAY LIST

-- <<ENTER NEXT COMMAND>>

SHEAR DIFFUSION IN SANDWICH SPECIMENS HAVING GLASS REINFORCED PLASTIC FACE PLATES WITH PAPER HONEYCOMB CORES

by

A. M. AHMAD MUSTAPHA

and

C. K. LIEW

SUMMARY

This project is an investigation into the behaviour of a glass reinforced plastic (GRP) strap used to join the face plates of two separate GRP skinned, paper honeycomb sandwich specimens, subjected to tensile loads of up to 1.5 kN. Results from the tests indicate that strap length and thickness taper of the strap influences the load diffusion process. Specimen length was found to have very little effect. The theoretical model developed gave good but conservative correlation with the experimental results. Moduli of the specimen found from three point bending tests are Young's modulus of the face plates = 15000 N/mm^2; and shear modulus of the core = 10 N/mm^2. The paper honeycomb core used had a thickness of 8.8 mm with $\frac{1}{8}$ inch cell size. The average thickness of each face plate was 0.5 mm

CONTENTS

CONTENTS (Continued)

NOMENCLATURE

Symbols

E	Young's modulus
F	Internal axial forces
G	Shear modulus
I	2nd moment of area
L	Length
P	End loads
Q	Shear loads
R	Roots of auxiliary equation of differential equation
t_i	thickness of material i
q	shear flow
v	deflection of beam
τ	shear stress
ϵ	longitudinal strain
γ	shear strain

Subscripts

b, B	Bottom skin
c	Core
g	Glue
p	Skin where strap is located
s	Strap
(1)	Unstrapped region
(2)	Strapped region

1. INTRODUCTION

In recent years composite materials have been developed to such a stage of sophistication that they have been adopted for use in a variety of ways in aircraft primary structures. Their major virtue is that they combine strength with lightness. Also the designer is now in a position to dictate how his material should behave. He is able to design the material itself to meet the requirements of the structure.

The structural material considered in this project is a sandwich panel with laminated glass reinforced plastic (GRP) face plates and a paper honeycomb core. Glass is a very strong material, but is very susceptible to surface flaws which weaken it considerably. However, produced in the form of thin fibres and embedded in a resin matrix to protect its surface it becomes a very useful material.

A remotely piloted vehicle (RPV) currently under development uses this glass sandwich material extensively. It is proposed that the wings be built in two halves to be joined with a single GRP strap attaching only the outer face plates together around the section periphery at the wing centre. This project is concerned with the load into such a GRP strap joint.

It can be divided into two sections:-

(i) Experimental work to study the effect of strap lengths and thickness taper on the diffusion of spanwise load from the sandwich material outboard of the centre span into the load carrying strap at the centre-span. It is necessary to determine the elastic constants of the material before embarking on the main body of experimental work. The elastic constants of the material were determined by a simple three point bending test. The final results were: $E \approx 15$ kN/mm^2 (GRP face plate)

$G \approx 10$ N/mm^2 (paper core)

The main body of experimental work was conducted on tensile specimens cut at mid-length and then joined with a GRP strap on one skin. The specimens were instrumentated to enable measurement of the variation of strain (or stress) in the GRP face plates.

(ii) Theoretical modelling of the load diffusion process. The model considered only diffusion in the honeycomb core. The strap was idealized to a step change in the cross-sectional area of the top skin.

The model showed an exponential strain variation along the tension specimen which was also evident in the experimental results. However, the model tended to give a conservative picture of the diffusion process, i.e. the strains predicted by the model tended to be slightly greater than the experimental ones.

2. APPARATUS

2.1 Introduction

As outlined in Section 1 (i), the experimental exercise carried out can be divided into two sections. The instruments used and the specimens built are outlined below.

2.2 Determination of the Elastic Constants

2.2.1 3 Point Bending Rig (Refer to Fig. 1)

This device was constructed from mild steel in order to have a stable platform on which to perform the test. It is simply a support for the beam specimens. Provision was made to provide a transverse load at the centre of the beam. A dial gauge was placed on the central loading tower in order to record the deflections. Another two gauges were placed on the supports of the rig itself in order to record any sinking of the whole system.

2.2.2 Bending Test Specimens

These were cut from a large sheet of composite material. The beams were of a constant 50 mm width. The beam lengths ranged from 200 to 500 mm (see Fig. 2).

2.3 Tensile Tests

2.3.1 Avery Test Machine

This is a hydraulic testing machine with a maximum "daylight" of five feet. The load applied could be read off from a dial on the control panel. However, the jaws of the machine were initially designed to take cylindrical specimens so a serrated face plate was designed to fit over the jaws and grip the specimens.

2.3.2 Electrical Strain Measuring Instrumentation

(i) Tinsley 4907 SH Bridge

The Tinsley unit is a manually operated strain gauge balancing bridge capable of giving readings down to two decimal places of percentage strain.

(ii) Apex Potentiometer Box

This potentiometer box was used to provide initial balance between the active gauge and the compensating gauge in each circuit. This had to be done so that direct strain readings could be read off from the Tinsley

unit during tests. The box is capable of providing switching for ten live gauges and their corresponding "dummies".

(iii) Type FLA-6-11 (4 x 6 mm) Strain Gauges

These strain gauges were purchased from Techni Measure Limited. They were manufactured by Tokyo Sokki Kenkyujo and their quoted gauge factor was 2.09.

2.3.3 Tensile Test Specimens

The structural material, i.e. the sandwich panel, was cut into standard 450 mm length, 50 mm width pieces. The core at one end of each piece was cut out over a length of 50 mm. This was then filled with a microballoon/epoxy mixture. Upon hardening of the epoxy, two aluminium face plates (50 x 50 mm) were attached, one either side, to this end, using Araldite resin.

The final test specimens were built up using these basic 450 mm length pieces. Two such pieces were butt-jointed at the unmodified ends using a strap, comprising laminations of glass tape with resin, laid on to one side (subsequently referred to as the upper or strapped skin). Two types of strap were used. Initially, the specimens were made using three laminations of glass tape/resin. A layer of resin was laid over one skin: then the glass tape strap was laid, covered with resin and allowed to cure before the next layer was laid. This was repeated for the other specimens.

A second batch of test specimens was also made up using only one layer of glass tape.

The specimens made are outlined in Table (1) and the basic layout of a typical specimen may be seen in Fig. 2.

The tapered straps simply had different lengths of glass tape in each layer as specified in Table (1). A 1400 mm specimen was also made in the same manner using two 700 mm long basic pieces.

Four 'core shear strength' specimens were made by cutting away, asymmetrically, one skin and core from each end of a 450 mm specimen. All the test specimens are illustrated in Fig. 2.

Finally, strain gauges were laid on the unstrapped or 'bottom' skin of the test specimens.

One gauge was placed 350 mm from the butt join and four other gauges were placed at discrete intervals between this gauge and the join.

One gauge was also placed on the strapped skin 350 mm from the join. This was to establish the datum strapped skin strain. The gauges were attached using C-N glue and their terminals were firmly soldered to thin copper wires.

3. THEORY

3.1 Introduction

This section is concerned with the development of the mathematical expressions used for this report. It will only briefly refer to the assumptions made and the resultant equations derived. Detailed derivations are included in the relevant appendices.

3.2 Calculation of Young's Modulus and Shear Modulus for the Sandwich Specimens

Consider a composite beam made up of GRP skins and paper honeycomb core. Since the honeycomb core is an antiplane material, it will have negligible stiffness along the length of the beam; so most axial loads will be taken up by the skins. Similarly, the shear stiffness of the glass skin in the depthwise direction is negligible compared to the core. Therefore, most shear loads will be taken up by the core at the interface between the core and the skin, all axial loads, shed by the skin, will be balanced by the complementary shear loads at the core. Using this principle and by considering a cantilevered beam with a tip shear load, an equation can be derived for the shear stresses in the core (see Appendix I).

This expression can now be applied to a composite beam subjected to 3 point bending. Any deflections will be the result of the superposition of deflections due to shear and bending loads. By considering each type of deflection case separately, and adding up the results, the resultant deflection v_R may be obtained. Thus

$$v_R = \frac{QL^3}{48\ EI} + \frac{QL\ t_c\ t_b}{8\ GI}$$

where bending deflection $= \frac{QL^3}{48\ EI}$ = function of E only

and shear deflection $= \frac{QL\ t_c\ t_b}{8\ GI}$ = function of G only

See Appendix II for the derivation.

Hence, finally, the manipulation of this equation and graphical means, will yield the required moduli, i.e. E for the face plates and G for the core. The method is outlined in Section 5.1.

3.3 Shear Diffusion Models

3.3.1 Loading Situation in Half Length, Shear Diffusion Specimen

All loads are based on unit width of specimen normal to plane of diagram.

Due to eccentricity of the load 2P in the strap, moments m and M_o will be generated to achieve moment equilibrium of the system. This will then cause bending curvature in the specimen.

If it is assumed that all bending curvature is small, then the above system may be separated into two components as indicated. These are not individually in equilibrium. Now as far as load diffusion is concerned, it is the system as shown in Fig. (ii) that really matters.

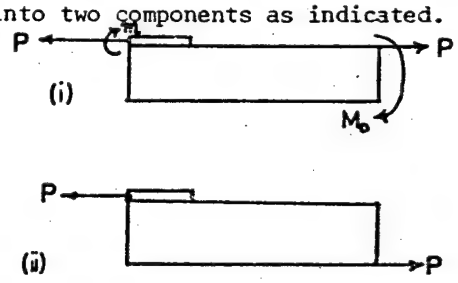

3.3.2 Shear Diffusion Model (see Appendix III)

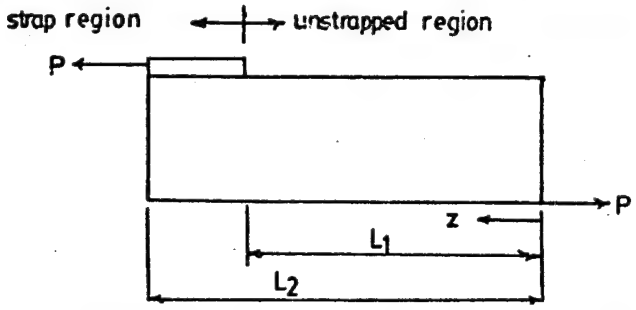

Expressions can be derived for axial strain in the lower skin at any station along the beam by splitting the beam up into two regions, namely the strapped and the unstrapped regions. Individual load diffusion equations derived for each of these two regions are 2nd order differential equations having the general solution of the form

$$\epsilon_B = b_1 e^{R_1 z} + b_2 e^{-R_1 z} + b_3$$ where b_i = constants

R_i = roots of the auxiliary equation of the differential equation.

Hence the longitudinal strain of the lower skin at any station can be completely described by

$$\varepsilon_B = \begin{cases} \varepsilon_{B1} = b_1 e^{R_1 z} + b_2 e^{-R_1 z} + b_3 & \text{unstrapped region} \\ \varepsilon_{B2} = b_4 e^{R_2 z} + b_5 e^{-R_2 z} + b_6 & \text{strap region} \end{cases}$$

The constants b_i can be found from the following boundary conditions for the lower skin at

(i) $z = 0$ $\quad \varepsilon_{B1}$ = strain due to load P; i.e. $\dfrac{P}{E\, t_b}$

(ii) $z = L_2$ $\quad \varepsilon_{B2} = 0$

(iii) $z = L_1$ $\quad \varepsilon_{B1} = \varepsilon_{B2}$

(iv) $z = L_1$ $\quad \dfrac{d\varepsilon_{B1}}{dz} = \dfrac{d\varepsilon_{B2}}{dz}$

3.3.3 Diffusion Model Where the Resin Which Attaches the Strap to Skin Forms a Shear Web

In the previous section, 3.3.2, it was assumed that the resin between the strap and skin had negligible thickness. In this model, it was assumed that the resin layer is important, and it forms a separate shear web. The resulting analysis yields a 4th order differential equation, whose solution is of the form

$$\varepsilon_B = a_1 e^{R_1 z} + a_2 e^{-R_1 z} + a_3 e^{R_2 z} + a_4 e^{-R_2 z} + a_5$$

When this equation was solved numerically, it was found that the roots R_1 were tending toward very large numbers (e.g. > 100), hence giving absurd results. The reason for this was not that the derivation was wrong but rather that the model was indicating that the whole system could be represented by just a 2nd order differential equation. This meant that the shear web of the glue was not important and hence it could be ignored. This was found to be consistent with physical results where thicknesses of glue were found to be around 0.1 mm.

4. PROCEDURE

4.1 Experimental Determination of the Elastic Constants of the Sandwich Material

These tests were performed on the apparatus described in (2.2.1). The test beam supporting frame was placed across two rigid supports.

The 200 mm test specimen was placed across the support rods and an initial load of 0.5 kg was applied in order to remove slack from the test system.

Loads ranging from 0.5 to 3 kg in increments of 0.5 kg were then applied. The deflections at mid span and at the two supports were recorded for each load case. This sequence was repeated for the 300, 400 and 500 mm specimens.

4.2 Tensile Tests on the Strapped Specimens

The tensile specimens used are outlined in Table 1. The basic tensile test will now be outlined in detail. Initially, the Tinsley bridge, the apex potentiometer and the measuring and compensating strain gauges were connected as shown in Fig. 3.

Before commencing the tensile test the measuring gauges were balanced using the apex variable potentiometers.

The specimen was then placed in the jaws of the Avery test machine. Loads varying from 0.6 kN to 1.5 kN were applied to the specimen. At each load the strain gauge bridge was again balanced, for each channel in turn, and the strain readings recorded.

This was repeated for the other test specimens.

Finally, comparisons of the failure strengths of the various strap length specimens and the special core shear strength specimens were made. This was accomplished by loading the specimens until failure. The failure load was recorded for each test case.

4.3 Computing

A computer program, in Basic Language, was written to help evaluate the theoretical strain equations derived. A flow chart, shown in Fig. 4, describes its operation. The equation evaluated is:

$$\epsilon_B = \begin{cases} \epsilon_{B1} = b_1 e^{R_1 z} + b_2 e^{-R_1 z} + b_3 & \text{unstrapped length} \\ \epsilon_{B2} = b_4 e^{R_2 z} + b_5 e^{-R_2 z} + b_6 & \text{strapped length} \end{cases}$$

Basic Language was used instead of Fortran because the evaluation required only a simple iterative calculation of the above equations.

5. RESULTS

5.1 Experimental Determination of the Elastic Constants of the Sandwich Material

A series of three point bending tests was carried out to determine the elastic constants. The mid-point deflection of a specimen due to a transverse load applied at the mid-point itself is given by the expression

$$v = \frac{QL^3}{48\,EI} + \frac{QL\,t_c\,t_b}{8\,IG} \text{ (see Appendix II)}$$

Manipulation of this equation gives

$$\frac{v}{QL} = \frac{1}{48\,EI}(L^2) + \frac{t_c\,t_b}{8\,IG} \quad \ldots\ldots\ldots\ldots\ldots (1)$$

$$\frac{v}{QL^3} = \frac{1}{48\,EI} + \frac{t_c\,t_b}{8\,IG}\left(\frac{1}{L^2}\right) \quad \ldots\ldots\ldots\ldots\ldots (2)$$

Plotting the total mid-point deflections against the applied loads yields Fig. 5. From this figure $\frac{v}{Q}$ is obtained as the slope of the straight lines. $\frac{v}{QL}$ and $\frac{v}{QL^3}$ may then be calculated by dividing by L and L^3 respectively. Using equation (1) $\frac{v}{QL}$ is plotted against L^2 (Fig. 6). Young's modulus E, may then be calculated from the slope and the shear modulus G from the intercept.

The values obtained were:

$E = 15\ kN/mm^2$

$G = 10.157\ N/mm^2$

NB: E refers to the face plates and G refers to the shear core.

Using equation (2), $\frac{v}{QL^3}$ is plotted against $\left(\frac{1}{L^2}\right)$ (see Fig. 7). This yields E from the intercept and G from the slope. Whence:

$E = 15.5\ kN/mm^2$

$G = 9.7\ N/mm^2$

The mean values were taken and are presented below.

$E = 15.25\ kN/mm^2$	
$G = 9.928\ N/mm^2$	

5.2 Results of Tensile Tests

The figures presented were selected to show typical results for the range of load and strap cases considered. The strains along the specimens for all the cases showed an exponential type variation thus supporting the mathematical expressions obtained for the theoretical models.

5.2.1 Effect of Different Strap Lengths

Fig. 8 shows typical diffusion curves for different strap lengths. The ordinate axis of this figure is in terms of percentage of load diffused into the upper skin. This is obtained from the formula:

$$\% \text{ load diffused} = \left(\frac{\varepsilon_{Bo} - \varepsilon_B}{\varepsilon_{Bo}}\right) \times 100$$

where ε_{Bo} = strain in lower skin at station where the loads in the upper and lower skins are equal

ε_B = local strain at any station on the lower skin

All the load in the lower skin was taken to have diffused into the upper skin at station 0 (i.e. the join between the two halves of the specimen). ε_{Bo} was arbitrarily taken as the average of the local strains in the upper and lower skins at station 350.

From the figure, it can be seen that the region where the load begins diffusing towards the upper skin is further away from the joint for the longer strap lengths. This clearly follows from the fact that, for the longer strap lengths, more load has been diffused to the upper skin at any station compared with a shorter strap specimen.

5.2.2 Effect of Thickness Taper of the Strap

The only effect observed was the influence which thickness taper has on the point where the load in the lower skin begins to diffuse into the upper skin. The load in the lower skin for the untapered strap cases begins diffusing into the upper skin further away from the joint at mid-span (see Figs 9 and 10). A tapered strap, in fact, behaves as a shorter untapered strap.

5.2.3 Effect of Increasing Specimen Length

Fig. 11 shows the variation of strain in the lower skin for different specimen lengths. The specimens both had a 400 mm strap length. It can be seen that the length of the specimen does not affect the diffusion

process for the two specimens considered. However, there is a limit to this. If a shorter specimen is taken (e.g. 600 instead of 900 mm specimens) the strain rate would, of course, be higher and the curve would be moved up above the 1400 mm curve.

5.3 Results from the Theoretical Model

These are shown in Figs 12 and 13 where a comparison was made with the experimental results. The figures indicate quite a good correlation but the mathematical model tends to give a higher rate of diffusion of load from the lower skin to the upper skin near the joint (station zero). This may be due to the fact that rather sweeping assumptions were made, making the model rather simplistic (e.g. ignoring bending moments and deflections in the specimen).

In the real case these may have a moderating influence on the rate of diffusion of load from the lower to upper skins. However, the model gave better correlation for longer strap length specimens.

The theoretical point where the load in the lower skin begins to diffuse to the top skin is shown in Fig. 14. This point was taken to be where the local strain reading differs from the initial strain readings (at the ends where the loads in the upper and lower skins were taken to be equal) by 0.01% strain. The figure indicates that this point occurs further away from the joint for longer strap lengths; this ties in very well with the inference made earlier in Section 5.2.1.

5.4 Destructive Testing

Table 3 indicates that the longer strap lengths have a higher failure load. Also, the core shear strength specimens seem to have approximately the same strength as the longer strap lengths (i.e. the 400 mm).

The single lamination specimens were found to have nearly the same failure strength as their triple laminated "brothers", e.g. the 200 mm strap (3 laminations) failed at 2.4 kN, while the 200 mm (single lamination) failed at 2.2 kN.

5.4.1 Failure in the Strap and Core

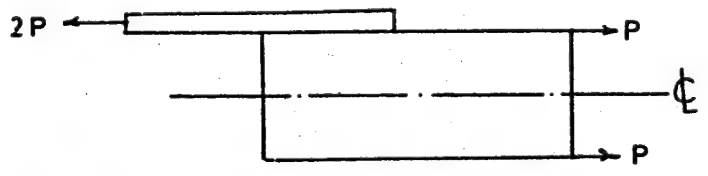

(a)

The figure above, Fig. (a), shows a section through the strap of a typical strapped specimen under load. Due to the geometry of the half specimen, the load case is asymmetric about the Neutral Axis (N.A.) of the sandwich. To try to re-establish symmetry of the loading system, the strap load 2P will tend to move down towards the centreline of the main body of the specimen as in Fig. (b).

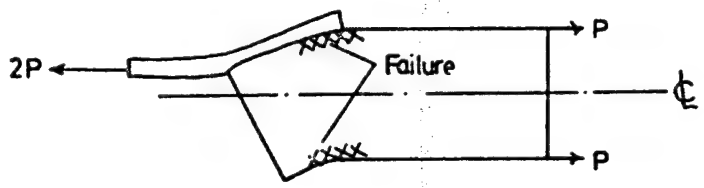

(b)

Failure occurs on the interface of the strap and the sandwich faceplates. There is also failure on the interface of the core and faceplates (see Fig. (b)). This was essentially failure of the glue bonding the strap, face plates and core together. No other type of failure was observed. The shear failure of the glue join occurred before damage to the core or failure of the face plates.

6. DISCUSSION

6.1 Experimental Results

As pointed out in Section 5.2.1, the longer strap lengths cause earlier diffusion of load from the lower skin to the upper skin. The reason why load is transferred from one skin to the other is that the axial strain in the lower skin is less than that in the upper. Assuming zero relative displacement at 350 mm from the join, the lower skin extension (moving towards the join) lags behind that in the upper skin giving rise to the shear strain in the core. The larger the 'lag' the greater the shear strain and hence the greater the rate of load transference between the skins.

The increased axial stiffness of the upper skin at the strap reduces the 'lag' in this region and, therefore, the load transference in the strap region. Since the total load to be transferred is the same (P) and the lag in the unstrapped region cannot suddenly be increased over that at the strap, the extent of the lag in the unstrapped region must increase to enable the remainder of the load (P) to be transferred.

This explanation can also be extended for the tapered strap cases. A tapered strap in effect behaves as a shorter untapered strap. Thus, the tapered straps would appear to act very much like the untapered straps near the join, but load diffusion across the core does not continue to quite such a distance from the join (Figs 9 and 10). This might be because the ends of the tapered straps are 'softer' being thinner, and the upper skin elongation here is increased slightly compared with the untapered strap.

For the two cases investigated, total specimen length was found not to have any great influence on the diffusion process. However, as mentioned earlier (Section 5.2.3) this would not be the case if a very much shorter specimen length were taken. If the loads remained constant the end strains (at the point where upper and lower skin loads were taken to be equal) would have to remain constant also. Thus the lower skin would experience the maximum strain at a point much nearer to the join. This would undoubtedly change the diffusion curve characteristics, (i.e. the load would have to diffuse faster from the lower to upper skins). Another likely possibility is that the upper and lower skin loads would not equalise in the length taken. The situation would then

be that the upper skin strains would be greater than the lower skin strains everywhere along the specimen.

The specimens with longer strap lengths seemed to possess a higher resistance to failure. This would appear to be expected because the upper skin is effectively thicker for a greater length. However, it seems likely that the real reason is that the shear strength in the resin between the strap and upper skin is critical (i.e. less than the tensile strength of a single glass lamination) so that increased shear area gives increased failure load. This interpretation is borne out by the fact that the strengths of single layer and triple layer straps were virtually the same for the same strap lengths and that failure ultimately occurred due to separation of the strap end from the upper skin (Section 5.4.1, Fig. (b)).

However, there was a good deal of scatter in the results suggesting that the epoxy/resin mix, curing time, humidity, etc. play an important role in the final determination of the failure strength of a specimen. The results presented in Table 3 are only typical values obtained from the tests.

6.2 Theoretical Model Result

In the GRP skinned paper honeycomb core specimens used, it is the strength of the bond between the face plates and the core which is critical in deciding the strength of the specimen. Thus the conservative prediction of lower skin strain by the mathematical model would lead to an overestimation of the load diffusion rates which, in turn, means an overestimation of shear stress in the core (see Appendix III, equation (3)). Therefore, this model can be used for design with confidence, but it must be realized that the model does not present a realistic and true picture of what is happening. In Section 3.3.1 the moments m and M_o and bending curvature were assumed to have secondary effects on the load diffusion process. Clearly from the results obtained, it seems to indicate that this assumption is not valid.

Now the whole specimen suffers from bending curvature. Hence the load in the strap can be resolved into two components, that is, along and perpendicular to the strap face plate.

The component perpendicular to the face plate is a shear force which will generate shear flows in the core which are in the same sense

as those in the system which 'diffuses' load from the lower to the upper skin.

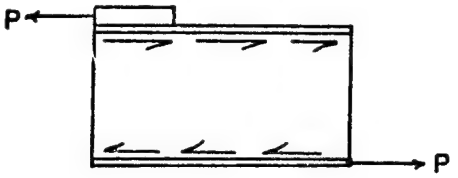

Shear Diffusion System

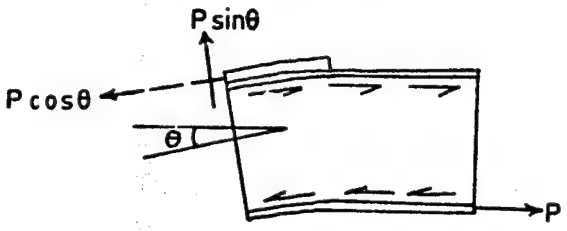

Shear Due to Bending Curvature

Hence bending curvature would result in the increase in core shear stresses which means an increase in load diffused from the lower to upper skin at any station, this possibly accounting for the discrepancies between the theoretical and measured values.

6.3 Possible Sources of Error

(i) The honeycomb material used was found to be not uniform. This may have affected the conditions along the specimens.

(ii) Since the strapped specimens were hand-made, there was almost certainly a variation in properties from one specimen to another. The epoxy resin composition and curing time were found to be important parameters in deciding the final specimen strength. Although great care was taken, it cannot be guaranteed that the above parameters were kept constant.

(iii) It was also found difficult to make the microballoon filler ends square. The microballoon filler tended to bulge out or contract in places thus changing the end geometry of the specimens. This may have affected the loading system within the specimen.

(iv) The Avery test machine proved hard to zero, so the load cases quoted may be slightly in error (not more than 1 kg zero error).

(v) Since the specimens were not entirely uniform it would be usual practice to test a large number of specimens, but the limited time available prevented this.

7. CONCLUSION

The mathematical model derived may be used in the design of the type of structures considered in this report, i.e. strap jointed sandwich structures. The model gives some overestimation of the strain rates near the join and hence the predicted shear stresses in this region are greater than those which develop in practice.

However, the model gives a better correlation for the longer strap length cases. To design for strength, it would be desirable to go for the longer strap lengths and, therefore, the model may be used in such design work.

An alternative would be to use tapered straps. Provided the length of the base layer were long enough, these straps would provide the required strength and also reduce material usage (maybe cutting costs).

REFERENCE

1. ALLEN HOWARD G. Analysis and Design of Structural Sandwich Panels
Pergamon 1969

ACKNOWLEDGEMENTS

The authors would like to take this opportunity to thank Mr R. P. Boswell for his infinite patience and help in the preparation of this report.

We would also like to thank Ann Ditcher and the technicians in the Aeronautical Laboratory for their assistance, and Mrs P. Packham for typing this report.

TABLE 1 TENSILE TEST SPECIMENS

Specimen	Length (mm)	Strap Length (mm)
1	900	100
2	900	200
3	900	300
4	900	400
5	900	400/450/300
6	900	400/200/100
7	900	200/100/50
8	1400	400
9	450	Shear Strength Specimen*
10	900	100†
11	900	200†
12	900	300†
13	900	400†

TABLE 2 MATERIAL CONSTANTS

	Thickness (mm)	Modulus (N/mm^2)
Strap	0.25 per layer	-
Skin	0.5	15000
Core	8.8	10**
Glue	0.1	1500**

TABLE 3 FAILURE LOADS

Specimen	Failure Load (kN)
2	2.4
3	4.4
9	4.0
11	2.2
12	4.3

*4 were made †single lamination strap **shear modulus

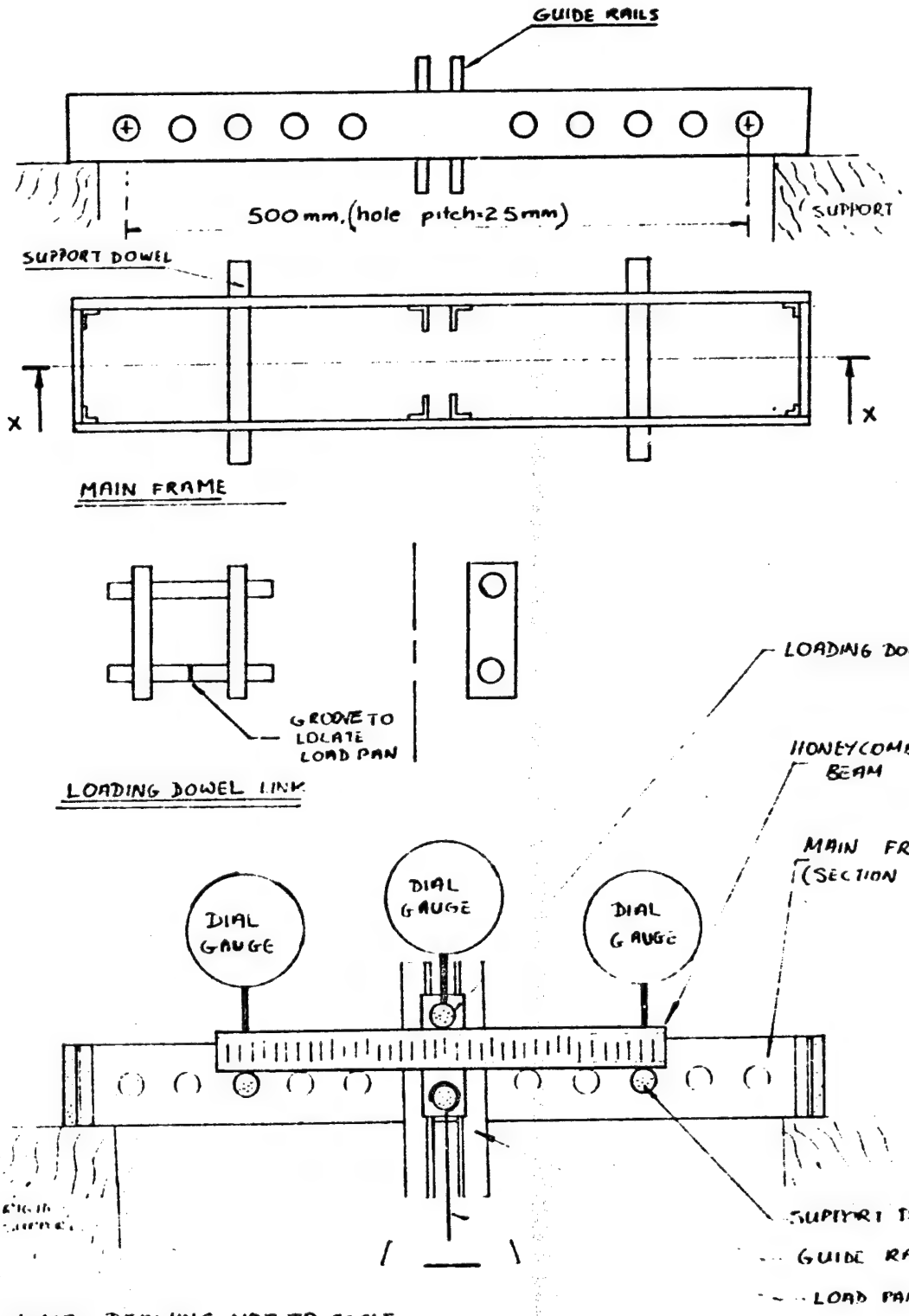

*NB: DRAWING NOT TO SCALE

NOTE : ALL DIAL GAUGES LOCATED ON A SUPPORT FROM MAIN FRAME SEPARATE

FIG 1

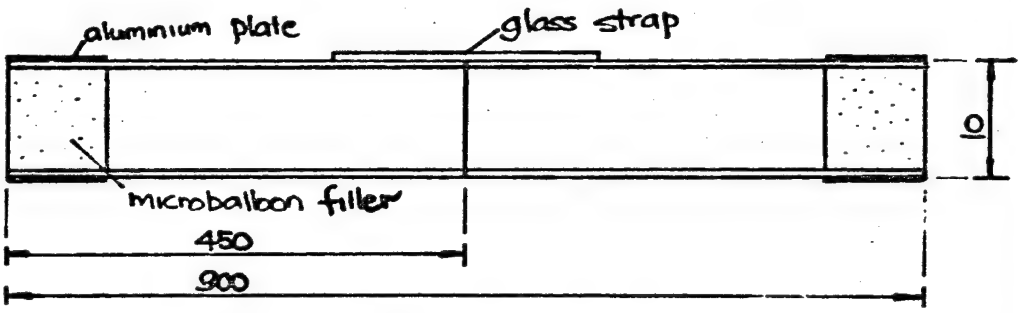

(i) Typical Tensile Test Specimen

(ii) Typical Bending Test Specimen

(* NB All dimensions in mm)

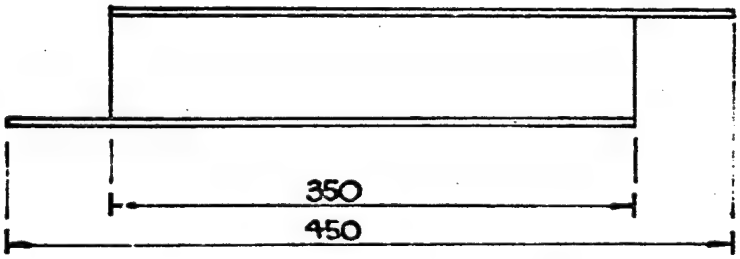

(iii) Core shear strength test specimen

Fig 2. Test Specimens (all specimens 50 mm wide)

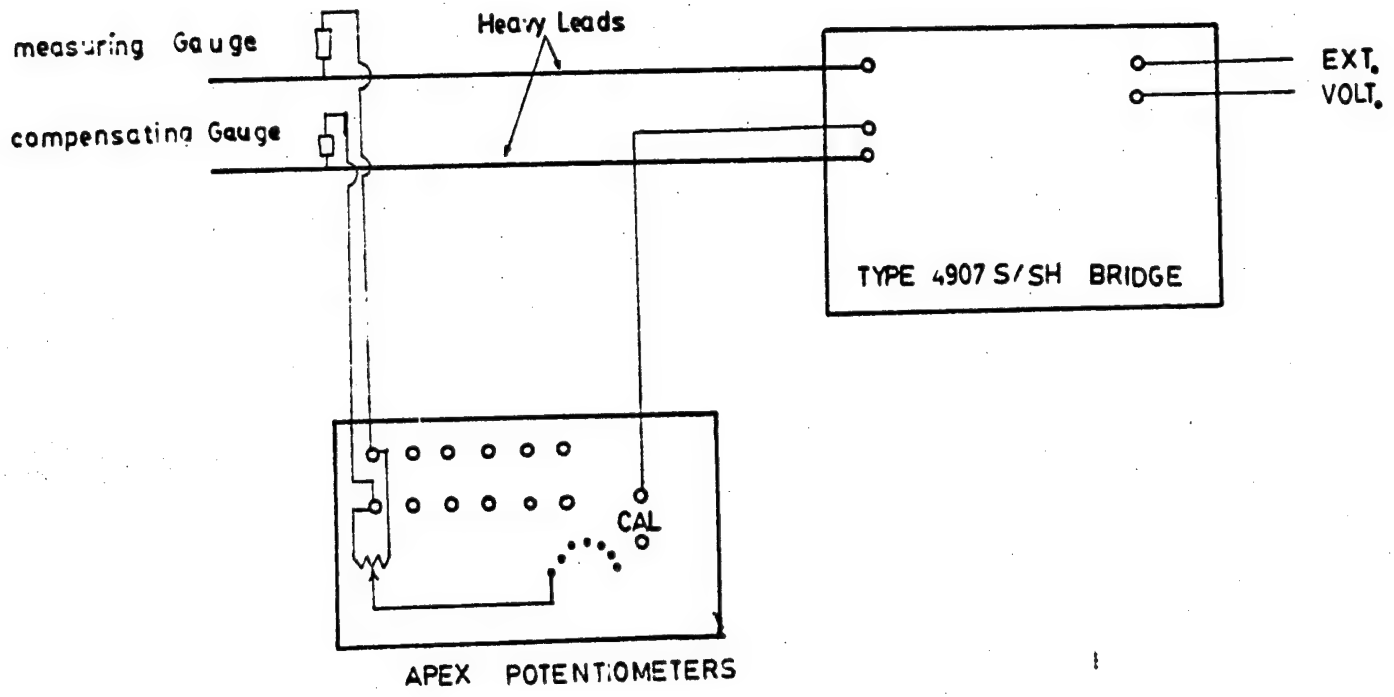

Fig 3 Curcuit Diagram for Tinsley Bridge

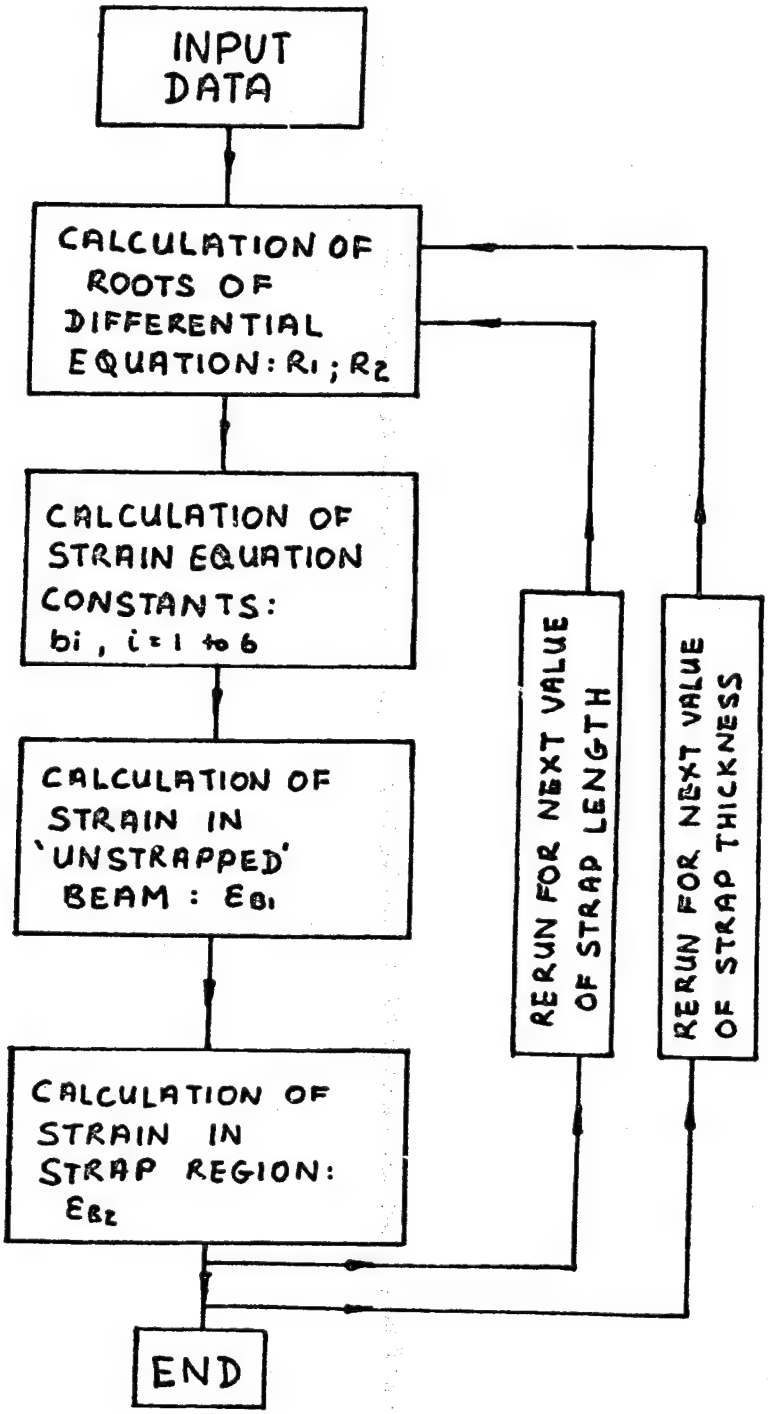
INPUT DATA
CALCULATION OF ROOTS OF DIFFERENTIAL EQUATION: R_1 ; R_2
CALCULATION OF STRAIN EQUATION CONSTANTS: b_i , $i = 1$ to 6
CALCULATION OF STRAIN IN 'UNSTRAPPED' BEAM : ε_{B1}
CALCULATION OF STRAIN IN STRAP REGION: ε_{B2}
RERUN FOR NEXT VALUE OF STRAP LENGTH
RERUN FOR NEXT VALUE OF STRAP THICKNESS
END

FIG. 4

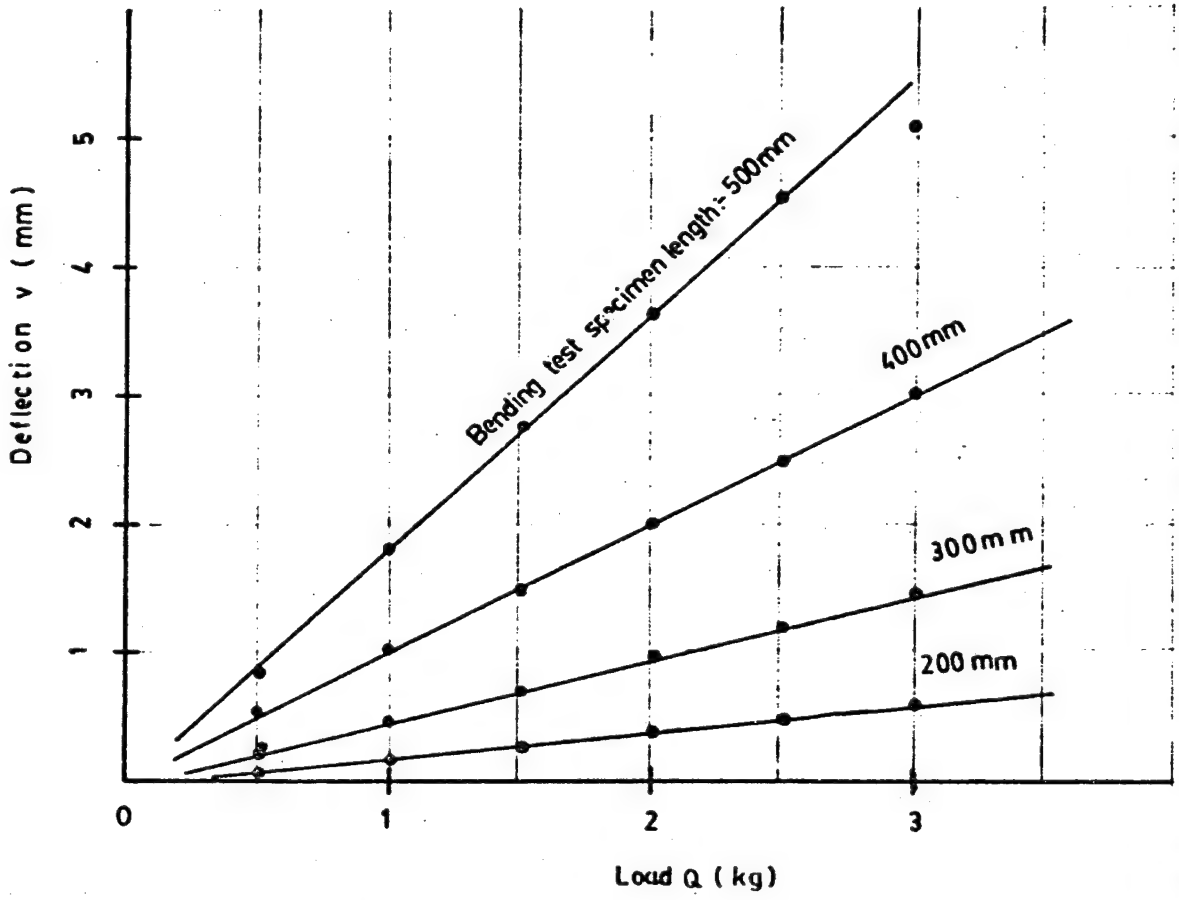

Fig. 5 Total deflection at mid-span

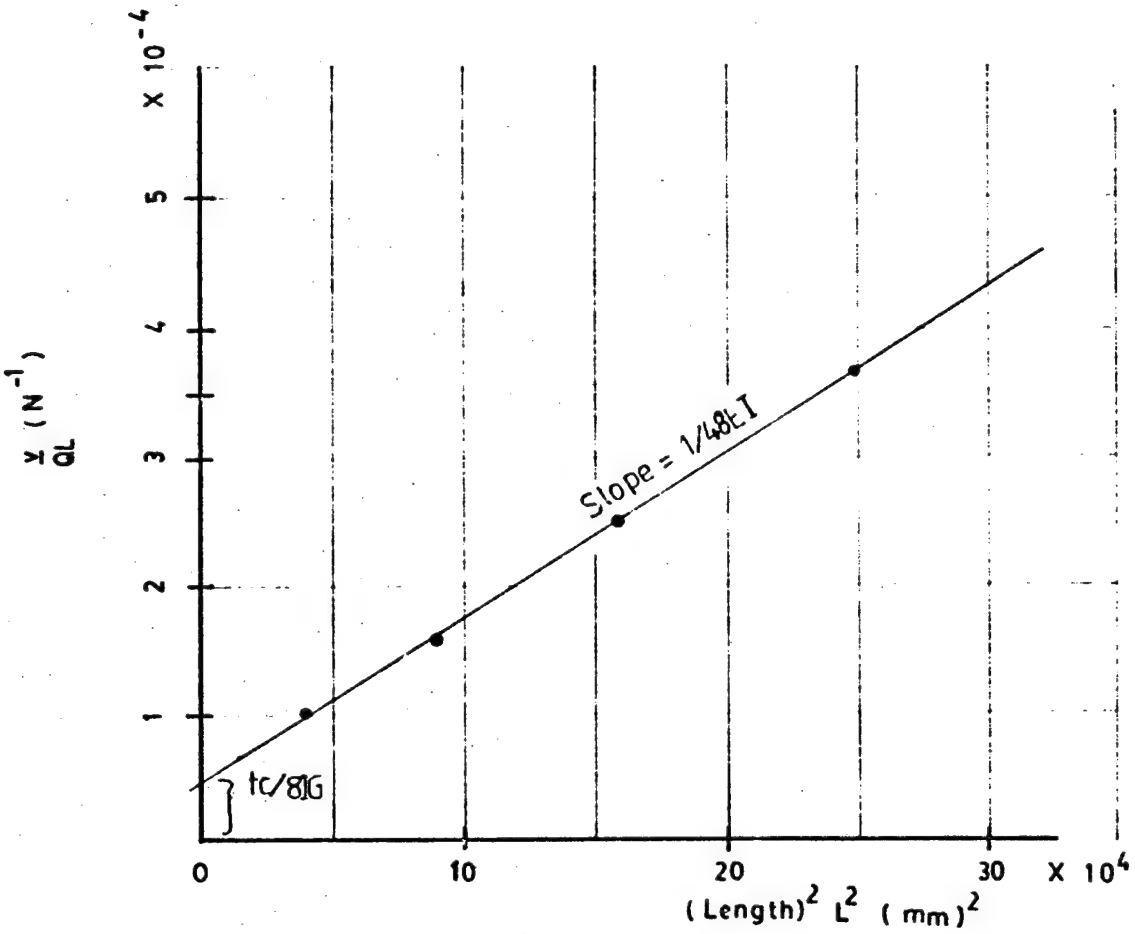

Fig 6 Determination of Mechanical Constants

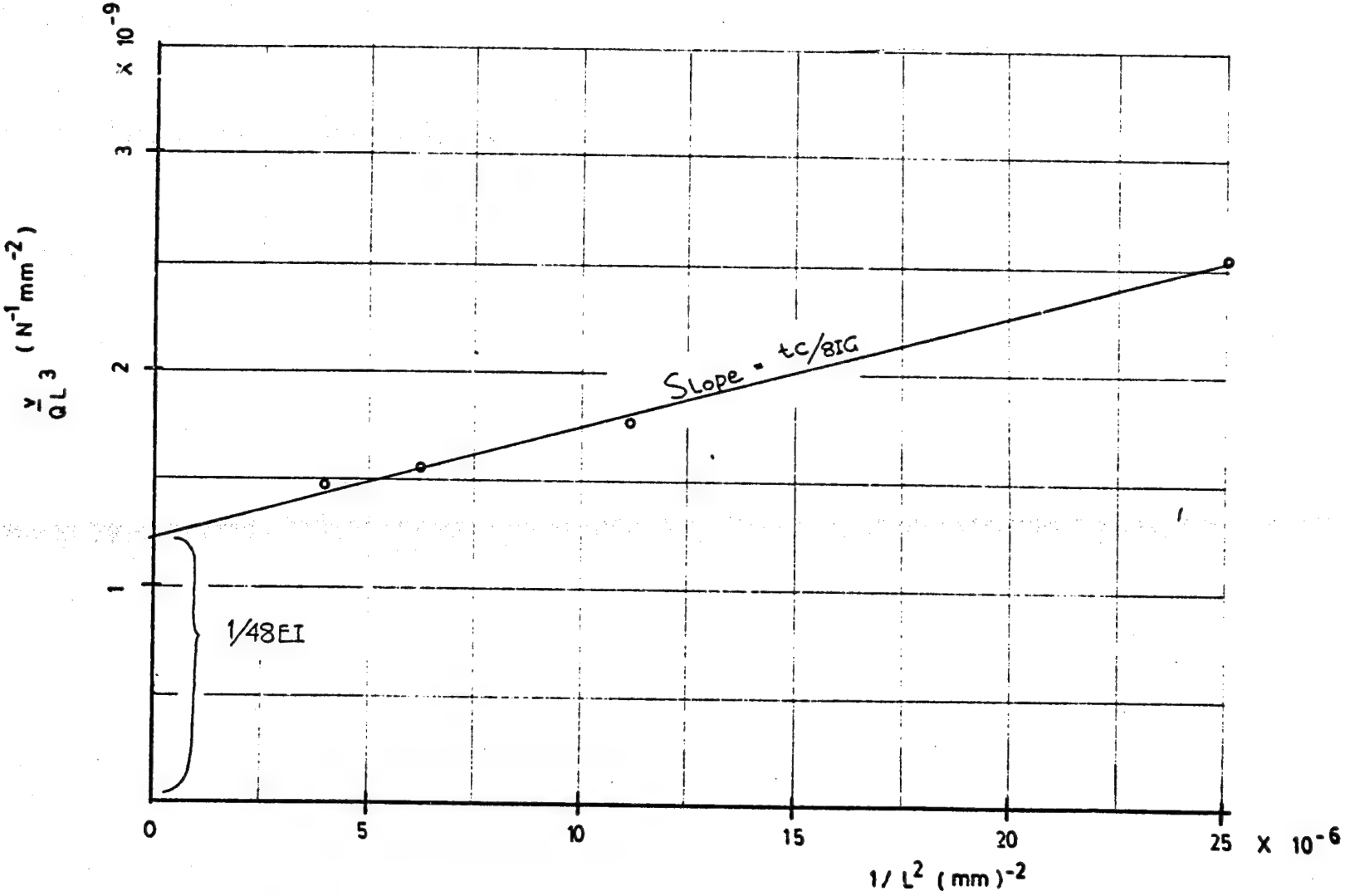

Fig 7 Determination of Mechanical Constants

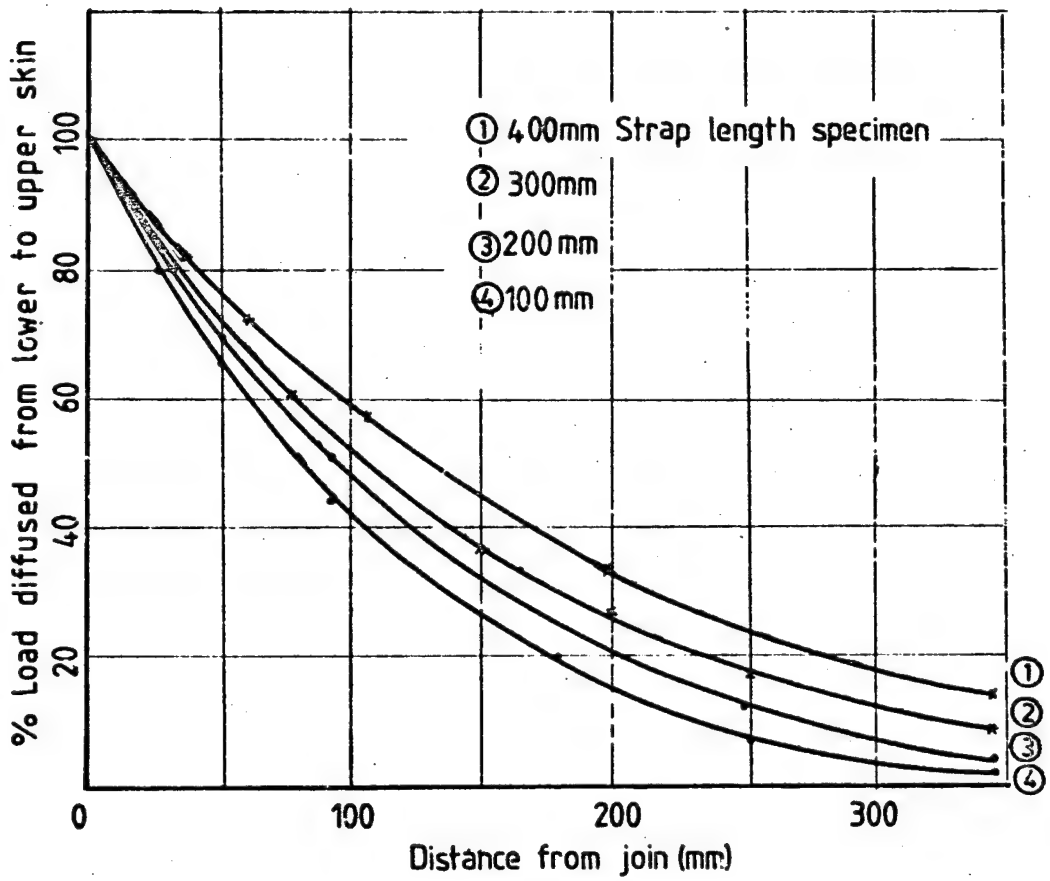

Fig.8 Diffusion along specimen

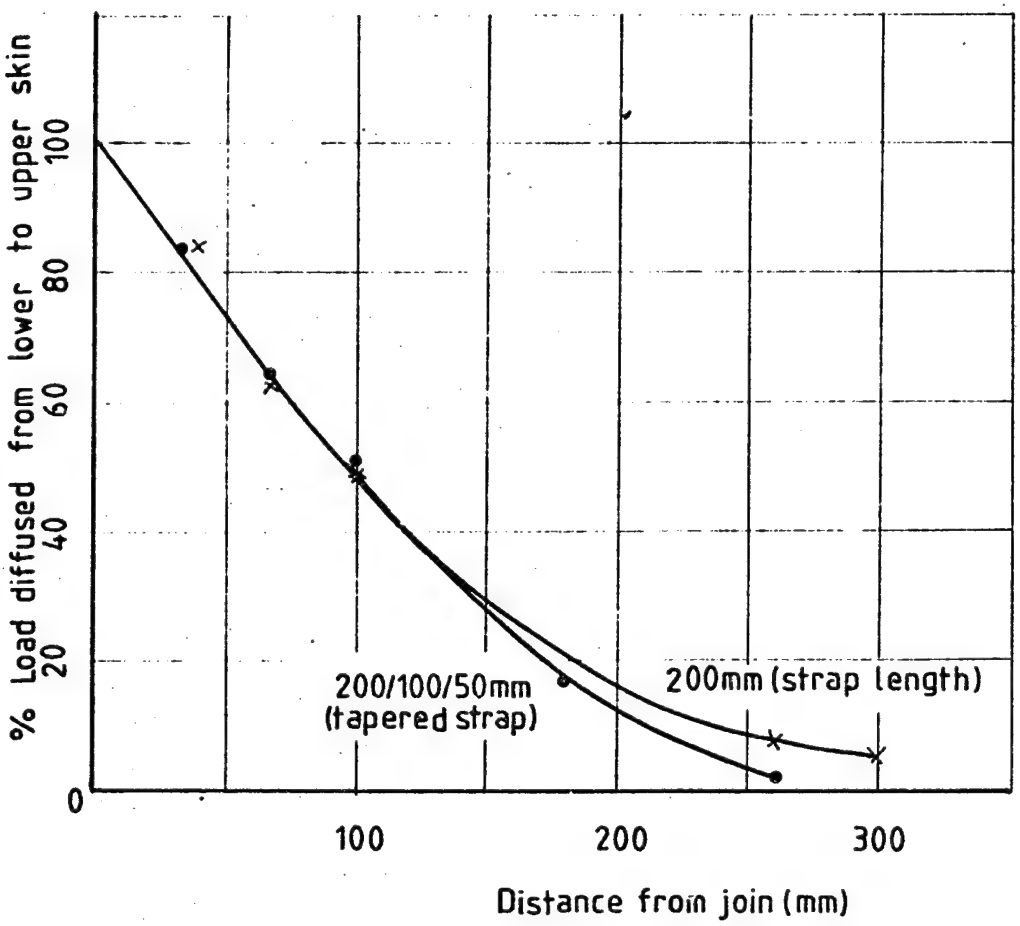

Fig.9 Effect of taper on load diffusion

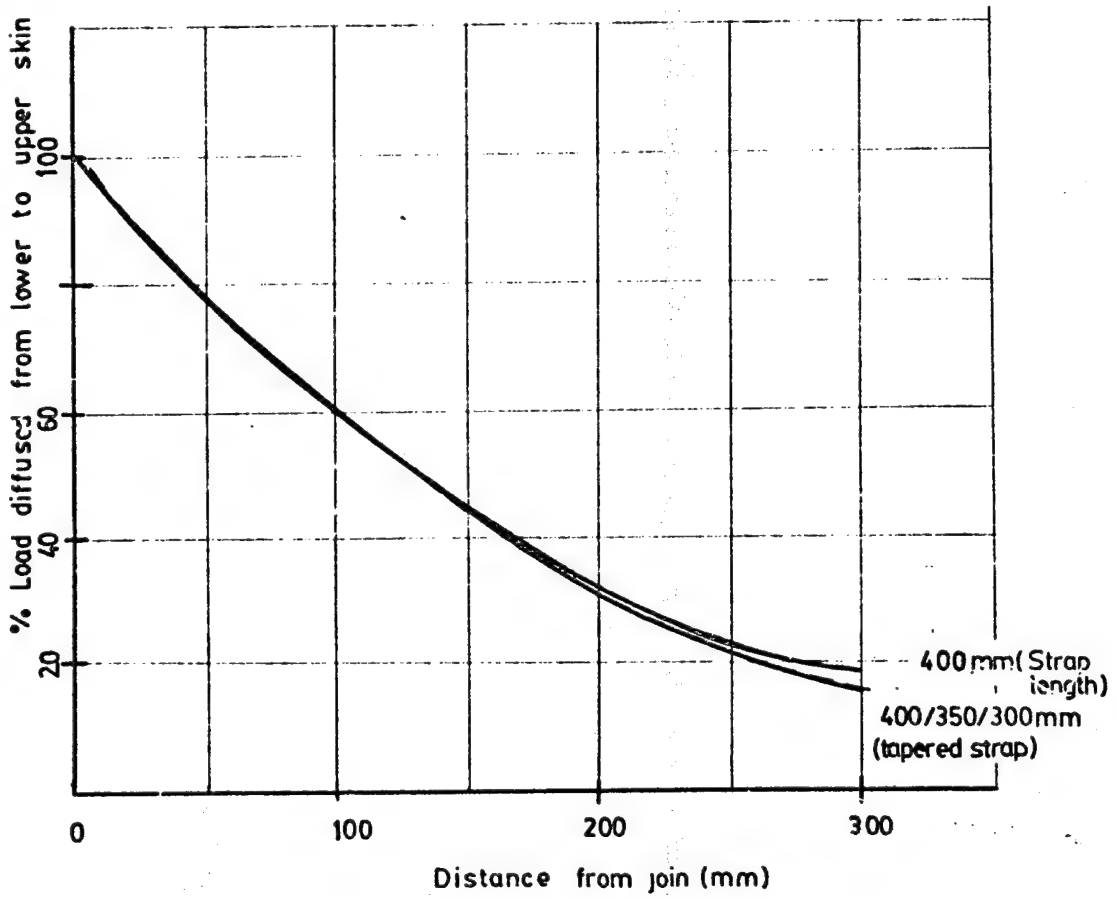

Fig 10 Effect Of Taper on load diffusion

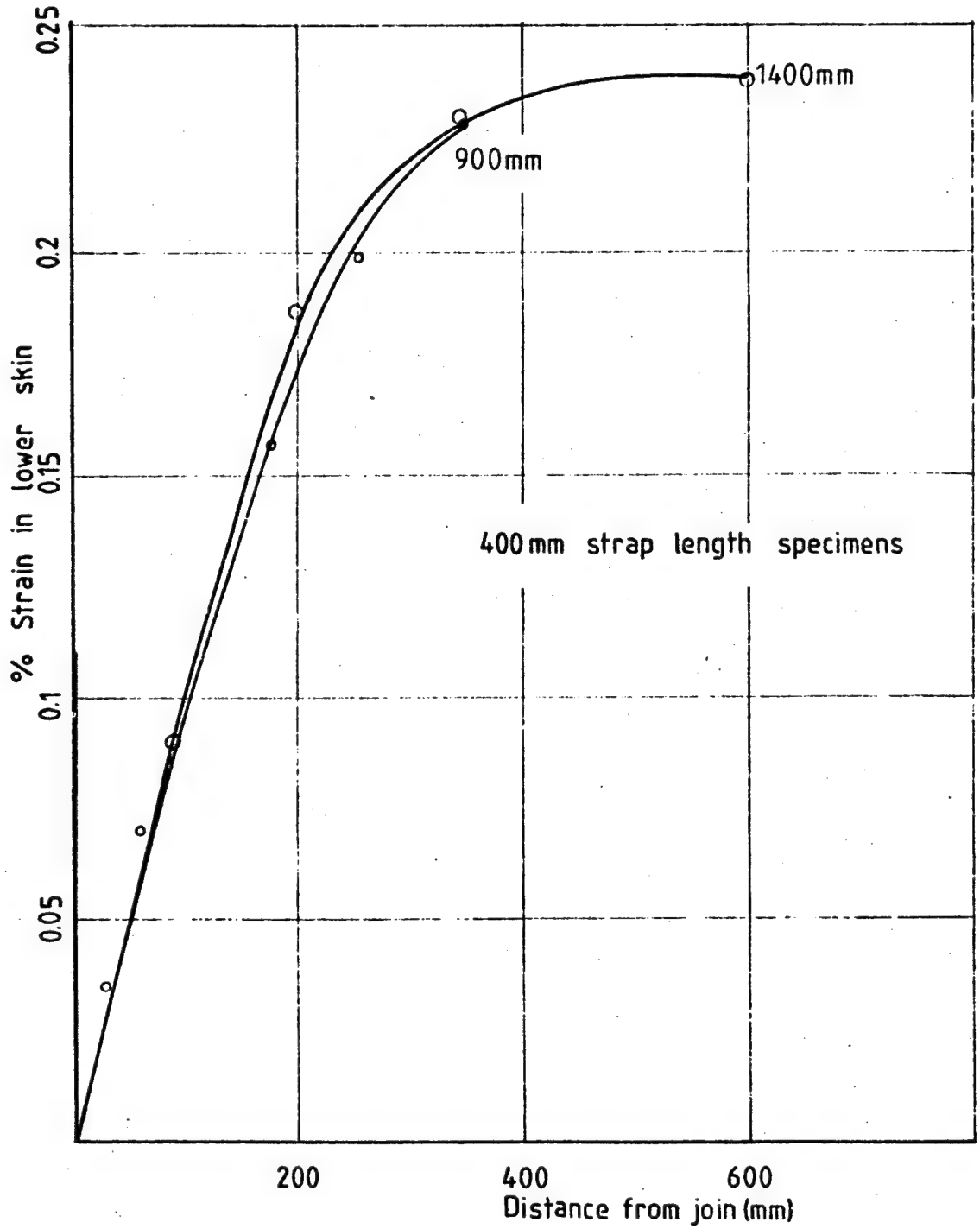

Fig.11 Comparison of the 1400mm & 900mm Specimens.

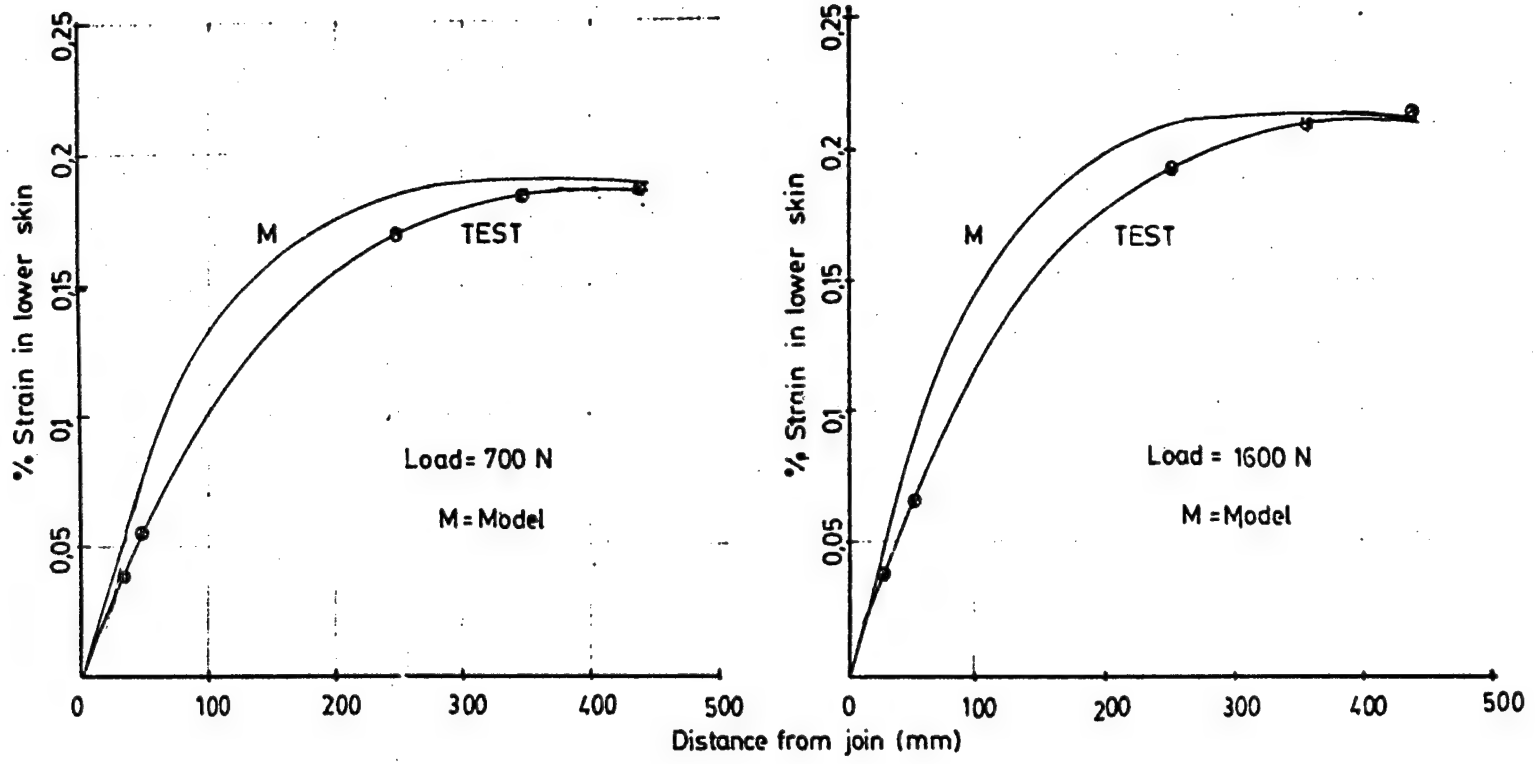

Fig. 12 Comparison of theoretical & experimental curves for a 100mm strap length specimen

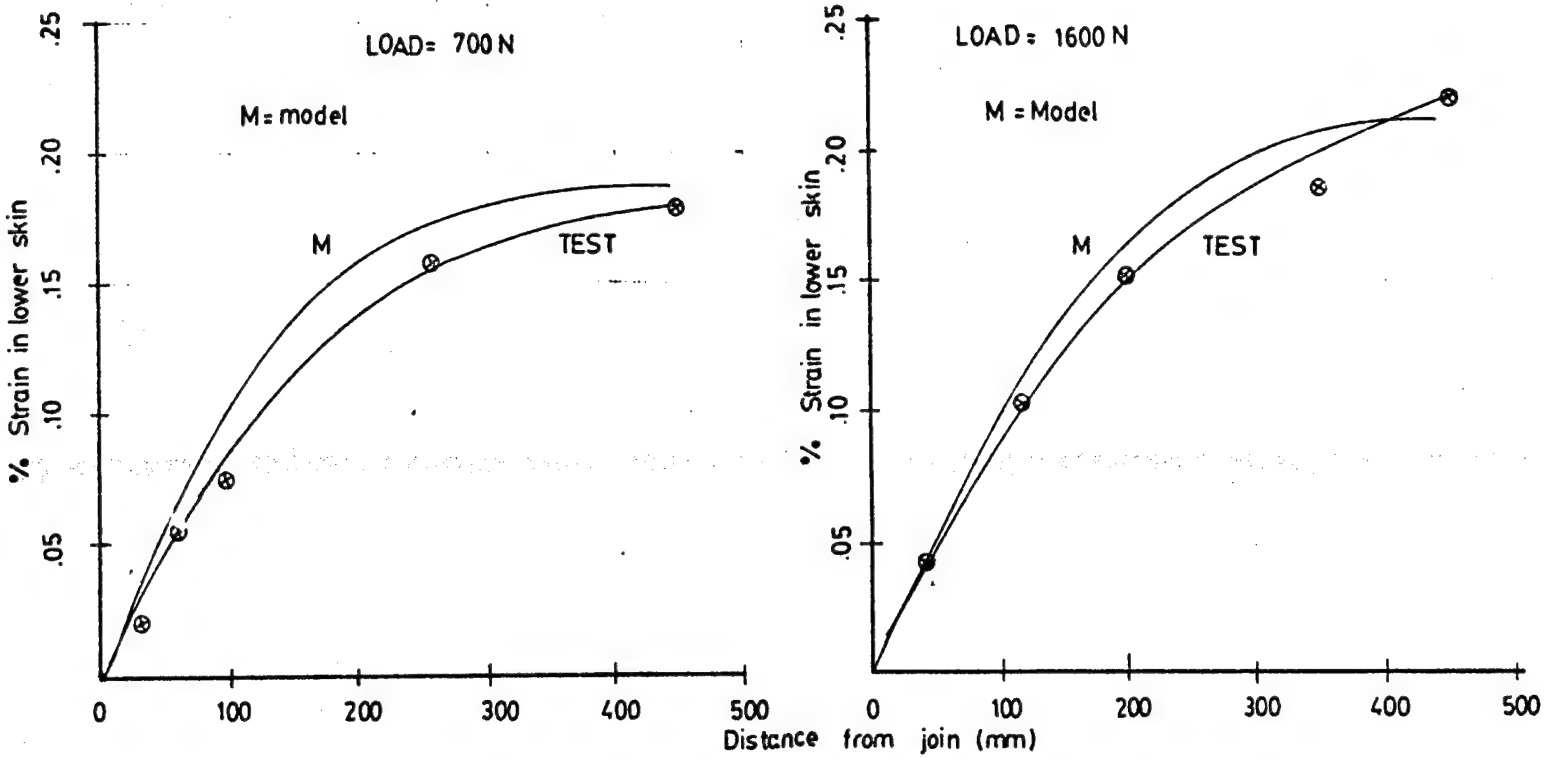

Fig. 13 Comparison of theoretical & experimental curves for a 400 mm strap length specimen

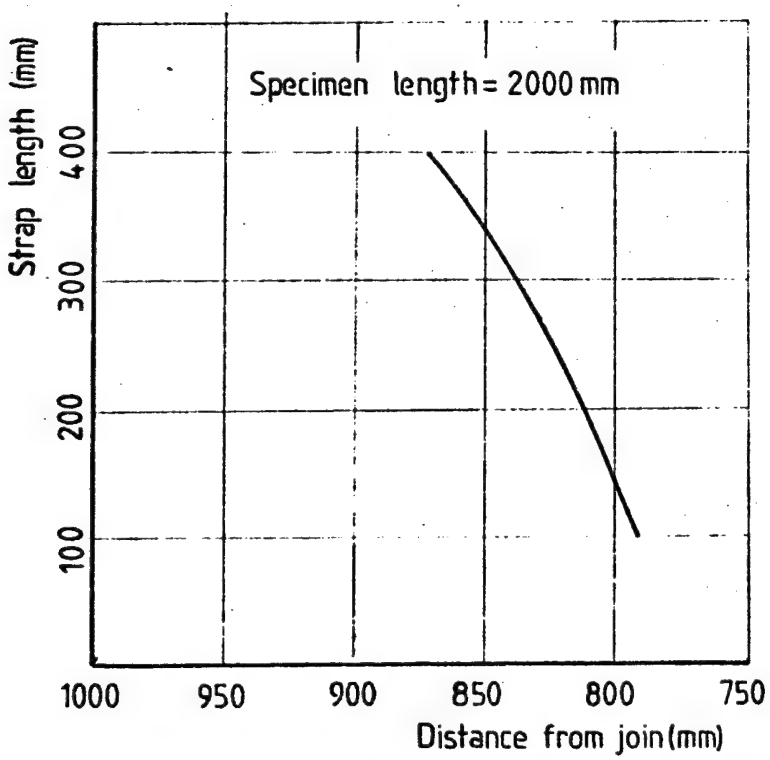

Fig 14 Theoretical point where load begins diffusing from lower to upper skin

APPENDIX I To find the Shearing Stress in Core. (Ref. 1)

Figure shows a cantilevered beam with a shear load Q as shown.

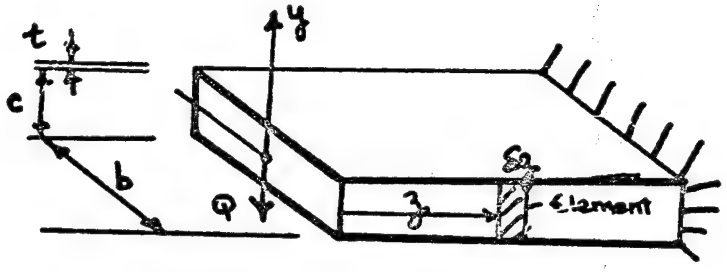

Consider an element length δz as shown. The element is at a distance z from the free end.

Taking moments at element

$$M = Qz \quad \text{——} (1)$$

Using Engineer's Theory of Bending

$$\frac{M}{I} = \frac{E}{R} = \frac{\sigma}{y}$$

$$\sigma = \frac{My}{I} = \frac{Q}{I} y z \quad \text{——} (2)$$

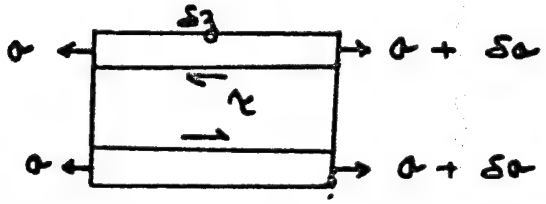

Considering equilibrium of element itself.

$$\tau = \delta\sigma$$

but from (2) $\delta\sigma = \frac{Q}{I} y \delta z$

∴ increment of tensile load = $\delta\sigma \times (b \times t)$

$= \frac{Q}{I} y \delta z (b \times t)$

This tensile load is equal to the shear load on interface of skin and cone.

$$\therefore \frac{Q}{I} y \, \delta z \, (b \times t) = \tau (b \times \delta z)$$

$$\Rightarrow \tau = \frac{Q}{I} y \frac{bt}{b}$$

$$= \frac{Q}{I} y$$

To obtain shear stress at the skin

$$y = \frac{1}{2}(c+t)$$

$$\therefore \tau = \frac{Qt}{2I}(c+t)$$

APPENDIX II SHEAR AND BENDING DEFLECTIONS

(Ref. 1)

Consider a beam under pure shear

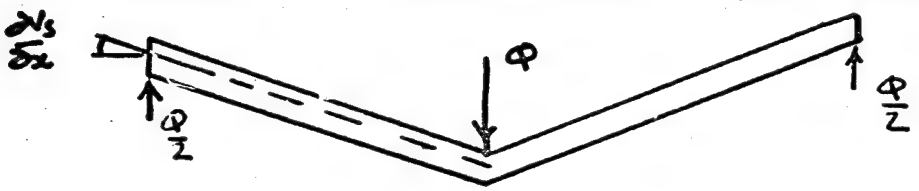

Taking an element of the beam

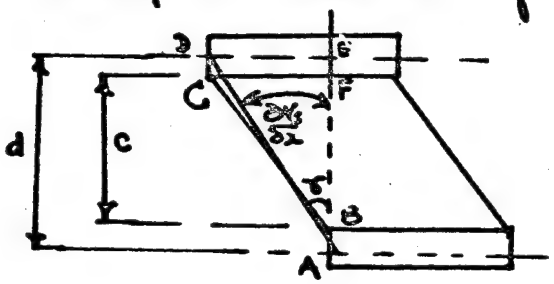

From geometry

$$DE = CF = \gamma c$$

But $DE = \left(\frac{\partial V_s}{\partial x}\right) d$

$$\therefore \gamma c = \left(\frac{dV_s}{dx}\right) d$$

$$\therefore \frac{dV_s}{dx} = \frac{\gamma c}{d} \quad \text{but} \quad \gamma = \frac{\tau}{G}$$

$$\therefore V_s = \int \frac{\tau c}{Gd}\, dx = \frac{\tau c}{Gd}\left[x\right]_0^{l/2}$$

$$= \frac{\tau c}{Gd}\left(\frac{l}{2}\right)$$

But $\tau = \frac{\bar{Q} t}{2I}(c+t)$ and $d = c+t$, $\bar{Q} = \frac{Q}{2}$

$$\therefore V_s = \frac{Qt}{4I}(c+t)\,\frac{cl}{2G}\,\frac{1}{(c+t)}$$

$$= \frac{Q\,t\,c\,l}{8IG}$$

This is the shear deflection term.

Now take a beam under pure bending. taking a section distance x from A.

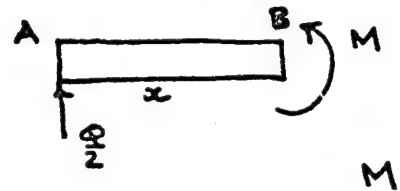

Taking moments at B

$$M = \frac{Q}{2}x$$

$$\therefore EI\frac{\partial^2 v_b}{\partial x^2} = -M = -\frac{Q}{2}x$$

$$EI\frac{\partial v_b}{\partial x} = -\frac{Q}{4}x^2 + C_1$$

when $x = \frac{l}{2}$ $\frac{\partial v_b}{\partial x} = 0$ $\therefore C_1 = \frac{Q}{16}l^2$

Integrating again $EI\,v_b = -\frac{Q}{12}x^3 + \frac{Q}{16}l^2x + C_2$

when $x = 0$ $v = 0$ $\therefore C_2 = 0$

At $x = \frac{l}{2}$ $EIv_b = -\frac{Q}{96}l^3 + \frac{Q}{32}l^3$

$$v_b = \frac{Ql^3}{48EI}$$

This is the bending deflection term.

APPENDIX III. SHEAR DIFFUSION MODEL

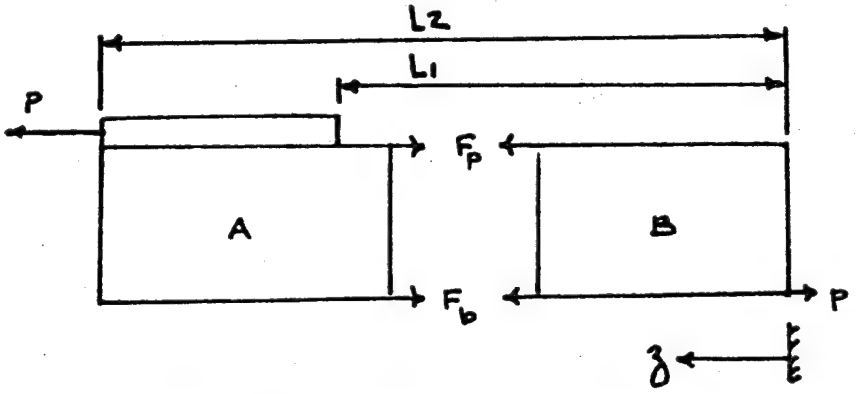

Axial Equilibrium of section A

$$F_p + F_b = P$$

Therefore at section $Et_p\epsilon_p + Et_b\epsilon_b = P$

where ϵ_p and ϵ_b are the strains of the top and lower skins respectively.

$$\therefore \epsilon_p = \frac{P}{Et_p} - \epsilon_b \quad (\text{as } t_b = t_p) \longrightarrow (1)$$

(1) Take an element in region $0 < z < L1$

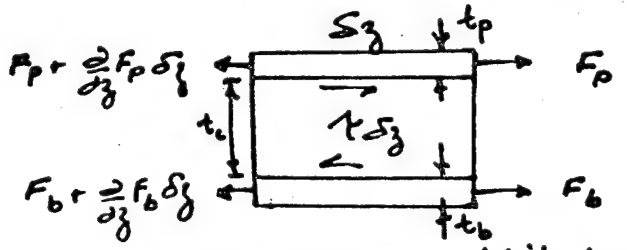

where F denotes Force / unit width.

Top skin equilibrium

$$\frac{\partial F_p}{\partial z} \delta z = \tau \delta z$$

$$\therefore \frac{\partial F_p}{\partial z} = \tau \longrightarrow (2)$$

Lower skin equilibrium

$$\frac{\partial F_b}{\partial z} \delta z + \tau \delta z = 0$$

$$\therefore \frac{\partial F_b}{\partial z} + \tau = 0 \longrightarrow (3)$$

Adding ① and ②

$$\frac{\partial F_p}{\partial z} = -\frac{\partial F_b}{\partial z} \quad \text{——④}$$

Consider equation ③

$$\frac{\partial F_b}{\partial z} + \tau = 0$$

but $\tau = G_c \gamma_c$; substitution into ③ gives

$$G_c \gamma_c = -\frac{\partial F_b}{\partial z} \quad \text{——⑤}$$

But $F_b = E t_b \epsilon_b$

$$\therefore G_c \gamma_c = -E t_b \frac{\partial \epsilon_b}{\partial z}$$

$$\frac{\partial \gamma_c}{\partial z} = -\frac{E t_b}{G_c} \frac{\partial^2 \epsilon_b}{\partial z^2} \quad \text{——⑤}$$

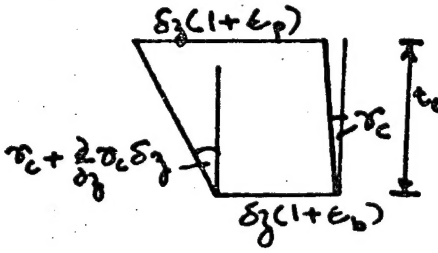

Compatibility

Now consider compatibility of strains in element under shear.

length(lower skin) = length(upper skin) − change due to shear.

$$\therefore \delta z(1+\epsilon_b) = \delta z(1+\epsilon_p) - t_c \frac{\partial \gamma_c}{\partial z}$$

$$\therefore \frac{\partial \gamma_c}{\partial z} = \frac{\epsilon_p - \epsilon_b}{t_c} \quad \text{——⑥}$$

Substitute into ⑤

$$\frac{E t_b}{G_c} \frac{\partial^2 \epsilon_b}{\partial z^2} + \frac{\epsilon_p - \epsilon_b}{t_c} = 0 \quad \text{——⑦}$$

Substitute for ϵ_p from ①

$$\frac{E t_b}{G_c} \frac{\partial^2 \epsilon_b}{\partial z^2} + \frac{P}{E t_p t_c} - \frac{\epsilon_b}{t_c} - \frac{\epsilon_b}{t_c} = 0$$

$$\therefore \quad \frac{\partial^2 \epsilon_b}{\partial z^2} - 2\frac{G_c}{E t_b t_c}\epsilon_b + \frac{G_c}{E t_b t_c}\frac{P}{E t_p} = 0 \qquad (8)$$

Solution is of the form

$$\epsilon_{b1} = a_1 e^{R_1 z} + a_2 e^{-R_1 z} + \frac{1}{2}\frac{P}{E t_p} \qquad (9)$$

where $R_1 = \sqrt{\frac{2G_c}{E t_b t_c}}$

(2) Now consider an element in region $L_1 < z < L_2$ (Now the strap is considered as part of the top skin.)

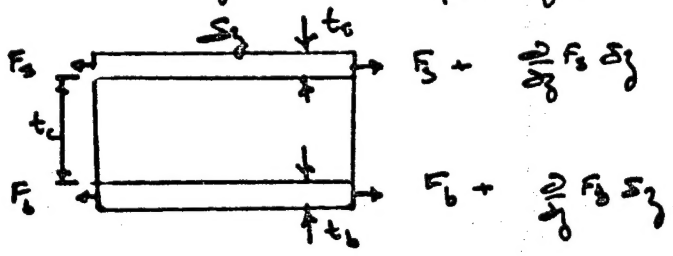

Equilibrium of lower skin

$$\frac{\partial F_b}{\partial z} = -\tau$$

$$E t_b \frac{\partial \epsilon_b}{\partial z} = -G_c \gamma_c$$

$$\frac{\partial \gamma_c}{\partial z} = \frac{E t_b}{G_c}\frac{\partial^2 \epsilon_b}{\partial z^2} \qquad (5)^*$$

This is similar to equation (5)

Compatibility leads us to a similar expression to (6) except with ϵ_s instead of t_p

ie $$\frac{\partial \gamma_c}{\partial z} = \epsilon_s - \epsilon_b \qquad (10)$$

Substitution into (5)*

$$\frac{E t_b}{G_c}\frac{\partial^2 \epsilon_b}{\partial z^2} + \frac{\epsilon_s - \epsilon_b}{t_c} = 0 \qquad (11)$$

Axial Equilibrium still holds

$P = F_s + F_b$ (similar to expression before except with F_s instead of F_p)

$\therefore E_s t_s \epsilon_s + E t_b \epsilon_b = P$

(where E_s denotes the Young's Modulus of the strap.)

$$\therefore \epsilon_s = \frac{P}{E_s t_s} - \epsilon_b \frac{E t_b}{E_s t_s} \qquad (12)$$

Substitute into (11)

$$\frac{E t_b}{G_c} \frac{\partial^2 \epsilon_b}{\partial z^2} - \left(\frac{E t_b}{E_s t_s t_c} + \frac{1}{t_c} \right) \epsilon_b = - \frac{P}{E_s t_s t_c}$$

This may be rewritten as

$$A \frac{\partial^2 \epsilon_b}{\partial z^2} - A_1 \epsilon_b = A_2$$

Solution is of the form

$$\epsilon_{b_2} = a_3 e^{R_2 z} + a_4 e^{-R_2 z} + a_5$$

where $R_2 = \sqrt{\frac{A_1}{A}} = \sqrt{\frac{G_c (E t_b + E_s t_s)}{E E_s t_s t_b t_c}}$

and $a_5 = \frac{A_2}{A_1} = \frac{P}{(E t_b + E_s t_s)}$

Thus at any section the strain of the lower skin may determined from

$$\epsilon_b \begin{cases} \epsilon_{b_1} = a_1 e^{R_1 z} + a_2 e^{-R_1 z} + \frac{1}{2} P / E t_p \\ \epsilon_{b_2} = a_3 e^{R_2 z} + a_4 e^{-R_2 z} + a_5 . \end{cases}$$

END

DATE

FILMED

FEBRUARY

1982